Quiz HD107 **Coastal Engineering**

Lucas M. Nogueira

PROBLEMS

Problem 1

A wave in water 120 m deep has a period of 8 seconds and a height of 3 m. True or false?

1.( ) The wavelength of the wave is greater than 105 m.
2.( ) The celerity of the wave is greater than 11 m/s.
3.( ) The steepness of the wave is greater than 0.02.
4.( ) The water particle speed at the wave crest is greater than 1.6 m/s.

Suppose now that the wave has propagated into a water depth of 12 m without refracting and without gaining or dissipating any energy. True or false?

5.( ) The wave height is now greater than 2.5 m.
6.( ) The water particle velocity at a point 1 m below the wave crest is greater than 1.6 m/s.
7.( ) The pressure at a point 1 m below the wave crest is greater than 25 kPa.

Problem 2

Part 1: A 5 m high, 8 sec period wave is propagating over a water depth that is just at the deep water limit. Using Stokes' theory, compute wave celerity and length. Also determine the wave crest and trough amplitudes. Compare the results to those of small-amplitude theory.

Part 2: Reconsider the wave described in the previous problem. Calculate the mass transport velocity for distances z below the water surface level such that $z = 0, -0.05, -0.1, -0.2, -0.3, -0.4$, and -0.5 times the wavelength. Compare this to the wave celerity and crest particle velocity.

▶ Problem 3

A shallow water wave has propagated to a nearshore depth of 2 meters. Its period is equal to 12 sec. The wave crests in deep water are oriented at an angle of 40° with the shoreline; the nearshore bottom contours are essentially straight and parallel to the shoreline. Determine the crest orientation and wave height with respect to the shoreline when the wave propagates into the abovementioned nearshore level.

▶ Problem 4

With reference to the following data, compute the total load sediment transport rate in a tidal current using the Ackers & White method and the van Rijn method. Assume that both methods apply to seawater just as they would for freshwater. Refer to the Additional Information section for the pertaining equations.

Tidal current, $\bar{u}$ = 2.5 m/s
Total shear velocity, $u_\star$ = 0.2 m/s
Grain size, D = 0.48 mm
Sediment specific gravity, G_s = 2.59
Water depth, h = 9 m
Seawater density, ρ = 1025 kg/m^3
Seawater kinematic viscosity, ν = 1.4×10^{-6} m^2/s

▶ Problem 5

Regarding various aspects of coastal science and engineering, true or false?

1.( ) The dimensionless fall velocity Ω, sometimes known as Dean's parameter, is based on a measure of sand transport potential and wave energy and is essentially an index of the ability of waves to move sand. A dissipative beach is generally associated with a lower Ω than an accretionary or steeper beach.

Macroalgae and macrophytes such as kelp have been shown to attenuate waves. As a consequence of the reduction of hydrodynamic energy, macrophyte vegetation may accumulate sediment and cause the water above the fore- and nearshore to become shallower. Such sediment accretion also contributes to coastal protection, since wave attenuation increases with decreasing relative water depth.

2.( ) However, Christianen *et al.* (2013) showed that the protective value of seagrass meadows is restricted to groups of high-canopy, high-aboveground-biomass algae; heavily grazed meadows, with their inherently small canopies and low aboveground biomass, offer no benefit in terms of coastal protection. ■

(A black square indicates the end of a multi-paragraph statement.)

Recommended research: Christianen *et al.* (2013).

3.( ) In a paper described as a 'warning for countries currently entering the process of coastal development', Pranzini (2018) reviewed the coastal management experience of Italy. He outlines the recent history of CM in that particular country and speaks of a 'sand age,' a period in which artificial deposition of sediment was massively implemented as a means of coastal protection and littoral restoration, to the detriment of the aggressive coastal defense-based program that had been the norm for many years before. On a national level, there remains a trend favoring reliance on beach nourishment; hard-engineering approaches such as groins have no place in contemporary Italian coastal practice.

Recommended research: Pranzini (2018).

Foredunes directly serve coastal communities by protecting lives, infrastructure, and ecosystems from inundation and erosion during severe storms; accordingly, conservation of these elements of coastal geomorphology has become a vibrant research topic in recent years.

4.( ) Mull and Ruggiero (2014) compared three models – a geometric model, an equilibrium profile model, and a wave impact model – as tools for foredune

erosion quantification in the context of the US Pacific Northwest. The models were evaluated in terms of their ability to replicate data obtained from a large-scale experiment and LiDAR data from the coasts of Oregon and Washington. Mull and Ruggiero (2014) concluded that the wave impact model was found to be the most applicable for estimating vulnerability to foredune erosion in the Pacific Northwest. ■

Recommended research: Mull and Ruggiero (2014).

McLachlan *et al.* (2013) developed a simple framework for assessing beach condition and suitability for different uses from which guidelines for planning, management and monitoring can be derived. They went on to propose two indices, namely a *Conservation Index* (CI) and a *Recreation Index* (RI), that together can be used to compare beaches and identify which areas (or sections of beach) should be demarcated for conservation, which for recreation and which for multi-purpose use.

5.( ) One important limitation of the CI/RI framework is that the original McLachlan *et al.* (2013) paper in which it was introduced offers no case studies or real world examples of application of this novel system. ■

Recommended research: McLachlan *et al.* (2013).

Reeve *et al.* (2008) noted that most coastal models available at the time had considered shoreline overtopping and overflow as separate phenomena. In view of this limitation, Reeve's group developed a numerical model to investigate the bulk qualities of combined overtopping and overflow in a free-surface turbulent flow, with emphasis on the behavior of discharge rate as a function of seawall slope, freeboard, and wavebreaking.

6.( ) Reeve's group conducted their numerical experiments using a Direct Numerical Simulation (DNS) scheme. ■

Recommended research: Reeve *et al.* (2008).

7.( ) Raubenheimer *et al.* (1995) employed a numerical model based on the depth-averaged nonlinear shallow water equations with bottom friction to model the surf and swash zones of a gently sloping beach. The numerics were then compared with observations in real environments. Importantly, Raubenheimer's group assessed the effect of inclusion of sea swell energy in the model runs and found that it can appreciably increase or decrease the amount of infragravity energy, sometimes by over 50 percent, not to mention its striking effect on the cross-shore energy distribution.

Recommended research: Raubenheimer *et al.* (1995).

8.( ) Hughes (1995) discussed how a modeler can establish a friction factor relevant for swash calculations while accounting for bed shear. To do so, Hughes resorted to Wilson's (1988) model for bed friction in the presence of sheet flow, which, Hughes observed, was warranted because sediment transport in swash motions occurred as sheet flow for most of the time. However, Hughes ultimately discarded the Wilson approach in favor of a different model because it yielded friction factors that deviated from Hughes' experimental estimates by several orders of magnitude.

Recommended research: Hughes (1995); Wilson (1988).

Until recently, reflection of incoming waves from coastal structures has been a largely underexplored topic, often no more than a byproduct of studies focusing on overtopping or structural stability. Zanuttigh and van der Meer (2008) attempted to remedy this in an extensive analysis of wave reflection data in European coasts, emphasizing, in particular, the development of a formula with which the wave reflection coefficient K_r can be determined.

9.( ) The formula developed by Zanuttigh and her colleague covers a wide variety of slope types and a wide range of breaker parameters ξ_0 with a simple equation that involves only two parameters. ■

Recommended research: Zanuttigh and van der Meer (2008).

Seawalls have long been used as a tool for coastal protection, but their effects on nearshore sedimentary processes remain poorly understood. Miles *et al.* (2001) used an *in situ* scheme to measure and investigate sediment dynamics in a shore defended by a sloping seawall. Instrumentation deployed included a pressure transducer and an optical backscatter sensor.

10.( ) One important advantage of the Miles *et al.* (2001) study is that sediment load and hydrodynamic measurements were carried out at several distances from the seawall. ■

Recommended research: Miles *et al.* (2001).

In addition to empirical formulas, wave reflection can be assessed using numerical models. One such approach is the use of artificial neural networks (ANNs), which Zanuttigh *et al.* (2013) employed to estimate the wave reflection coefficient from coastal and harbor structures under a variety of wave conditions; the reflection data used to train and develop the ANN were taken from Zanuttigh and van der Meer (2008), the same paper mentioned in statement 9.

11.( ) Zanuttigh's group used an ANN with more than 30 hidden neurons. ■

Recommended research: Zanuttigh *et al.* (2013).

Miller and Dean (2004) proposed a simple model for assessment of shoreline change and validated it with data from 10 sites in six US states. The model offers a reliable framework for the prediction of large-scale shoreline changes due to cross-shore processes, particularly on relatively straight, uninterrupted shorelines.

12.( ) In the Miller-Dean model, a shoreline approaches an equilibrium state linearly with time. In spite of its simplicity, the model is successful in predicting the correct *direction* of shoreline changes, albeit with some overprediction of the *magnitude* of the changes. ■

Recommended research: Miller and Dean (2004).

Yates *et al.* (2009) developed an equilibrium-type shoreline change model using 5 years' worth of observations from Torrey Pines Beach, California, and two nearby sites. The model successfully reproduces shoreline location for time periods not used in model calibration and can be used to predict beach response to past or hypothetical future wave climates. Later, Yates *et al.* (2011) applied the same model to a different California coast with higher sediment diameter and more energetic winter waves.

13.( ) One important feature of the Yates model is that shoreline contour displacement depends on wave energy rather than wave direction or alongshore gradients in waves and currents. ■

Recommended research: Yates *et al.* (2009); Yates *et al.* (2011).

Aagaard and Hughes (2006) studied the near-bed horizontal and vertical velocity structure and the ensuing sediment resuspension and transport in two dissipative beaches dominated by uprush/backwash at infragravity time scales. Importantly, Aagaard and his colleague used an explicit formulation of shear stress that dealt away with the usual friction coefficient × dynamic pressure product.

14.( ) Importantly, Aagaard and Hughes found that, in their novel approach, not only were functional relationships between bed shear stress and sediment load found to be reasonable, the parameters that related the two variables were found to be the same for the uprush phase and the backwash phase, conferring greater robustness to their model. ■

Recommended research: Aagaard and Hughes (2006).

15.( ) In recent years, coastal researchers have harnessed the exponential growth in computing power to develop increasingly more sophisticated numerical simulations, all the while diminishing reliance on semi-empirical

formulas such as the ones listed in the USACE's *Coastal Engineering Manual*. The supremacy of numerical solutions is exemplified in Guanche *et al.* (2009), who used a Volume-Averaged Reynolds-Averaged Navier-Stokes (VARANS) code named COBRAS-UC to simulate wave-induced loads on a low-mound breakwater and validate the results with data from laboratory and prototype scales; also included in the study were equivalent calculations with semi-empirical formulations from Sainflou (published in 1928), Nagai (published in 1973), and Takahashi *et al.* (published in 1994). Guanche's group reported that COBRAS-UC predicted wave loads on the breakwater with more accuracy than any of these three sets of semi-empirical correlations.

Recommended research: Guanche *et al.* (2009).

Hubbard and Dodd (2002) used a 2D nonlinear shallow water model to study wave runup and overtopping. Those authors demonstrated that their model, called OTT-2D, performs well both in idealized bathymetries and in more realistic situations with nonuniform, complex bathymetries that would've proven too computationally demanding for other codes available at the time.

16.( ) One important feature of the computational model used by Hubbard and Dobb is that it uses an adaptive grid. ■

Recommended research: Hubbard and Dodd (2002).

Shiach *et al.* (2004) used a finite-volume model based on the shallow water equations (SWE) to assess a series of experiments on overtopping of a near-vertical sloping structure under the effect of impacting waves. The experiments were conducted in the University of Edinburgh as part of the VOWS (Violent Overtopping by Waves at Sea) project.

17.( ) Comparisons between water surface elevations of the physical and numerical models showed that although waves occurred at similar times in both physical and numerical settings, the numerical surface tended to overpredict the heights of each wave. ■

Recommended research: Shiach *et al.* (2004).

18.( ) Park *et al.* (2017) used an extensive large-scale experimental dataset to analyze the effects of irregular wave loads on an elevated coastal structure. They assessed variation in horizontal and vertical wave forces, both of which may be crucial for coastal structure design. Although Park's group found that the forces caused by nonbreaking waves are large with respect to incident wave energy, their experimental structure recorded a larger horizontal force when subjected to breaking waves than when impacted by smaller, nonbreaking waves. In contrast, the specimen recorded vertical wave forces of similar order of magnitude for all wave conditions.

Recommended research: Park *et al.* (2017).

One important issue in nearshore discretization techniques is how to establish an appropriate representation of flow at the shoreward boundary of the domain. As summarized by Prasad and Svendsen (2003), there are at least two approaches in this regard. The first is the *fixed grid* approach, whereby the position of the shoreline is determined as a special point positioned between the last wet point and the first dry grid point; this is done by solving the momentum equation for a fluid particle at the shoreline. In the *coordinate transformation* approach, use is made of a coordinate transformation that maps the changing domain onto a fixed domain and solves the basic hydrodynamic equations in the mapped domain.

19.( ) Prasad and Svendsen put both methods to the test by assessing their performance in three well-known problems related to nonlinear shoreline motion. Both approaches performed well in validating the results from the three problems. ■

Recommended research: Prasad and Svendsen (2003).

Smoothed Particle Hydrodynamics (SPH) has recently emerged as an alternative to "traditional" numerical methods. Originally developed as tools for astrophysical modelling, SPH schemes are based on a Lagrangian framework and can be used to simulate free-surface flows with no need for a special treatment of the surface, which makes them particularly amenable for violent, rapidly-varying open flows of coastal interest. Aware of these features, Altomare *et al.* (2015) used a free SPH code called DualSPHysics to study wave loading on coastal structures. Crucially, Altomare's group validated DualSPHysics with classical problems of coastal engineering and went on to compare their wave-load model with similar simulations performed with the commercial program FLOW-3D.

20.( ) One advantage of DualSPHysics over FLOW-3D in coastal applications is that only the former is endowed with an active wave absorption system (AWAS). ■

Recommended research: Altomare *et al.* (2015).

Sugano *et al.* (2014) reported the extensive damage to Japanese coastal infrastructure as it was ravaged by the 2011 earthquake off the Pacific coast of Tohoku, in the northeastern part of the country. Sugano's group, working on behalf of Japan's Port and Airport Research Institute (PARI), investigated damage along approximately 600 km of coastline and conducted an extensive effort to distinguish damage to coastal structures resulting from strong ground shaking and secondary effects (e.g., liquefaction or ground failures) from that caused by tsunami inundation.

21.( ) Damage to coastal structures, Sugano's group argued, was minimal because Japanese coastal and geotechnical engineering practice has long been steeped on provisions that consider occurrence of earthquakes and tsunamis *in combination*, rather than unrelated phenomena. ■

Recommended research: Sugano *et al.* (2014).

22.( ) While it is well-established that coastal protection design heights will have to be modified (almost always, increased) in response to climate change-induced sea-level rise, there is yet no consensus on how to relate the dynamics of SLR (itself a heavily debated topic) to practical engineering issues. In one such effort, Arns *et al.* (2017), working with data from the German Wadden Sea, developed a hydrological model that predicts that coastal areas' design heights may have to be aggressively increased, sometimes by as much as 50%, if they are to withstand future SLR. One drawback of the Arns study, however, is that it relies exclusively on predicted SLR and does away with potentially relevant inputs such as variations in storm tides.

Recommended research: Arns *et al.* (2017).

23.( ) Vousdoukas *et al.* (2020a) argued that shoreline dynamics and coastal recession driven by sea-level rise could lead to the extinction of nearly half of the world's sandy beaches at the end of the present century. In a reply, Cooper *et al.* (2020) concurred with the findings reported by Vousdoukas's group and commended aspects of their methodology, such as reliance on the Bruun rule, presumption that coastal response to SLR always involves shoreline retreat, and omission of topography or the material nature of the basement over which the beach is migrating.

Recommended research: Vousdoukas *et al.* (2020a); Cooper *et al.* (2020); Vousdoukas *et al.* (2020b).

24.( ) In view of its fragile theoretical underpinnings, researchers studying coastal recession have begun to eschew the so-called Bruun rule, and a growing preference for probabilistic, risk-based techniques has taken hold. One example is the Probabilistic Coastline Recession (PCR) model introduced by Ranasinghe *et al.* (2012), which provides statistical estimates of coastal recession based on well-established physical processes. Ranasinghe's group calibrated their novel model with data from Narrabeen beach, Australia, and went on to analyze the

same site with the Bruun rule; in that case study at least, the Bruun rule offered highly conservative estimates of coastal recession.

Recommended research: Ranasinghe *et al.* (2012).

ADDITIONAL INFORMATION

Sediment transport with the Ackers & White and van Rijn methods (modified from Reeve *et al.*, 2004)

→ *Ackers and White method*

In the Ackers and White method of total load transport, three dimensionless parameters are used, namely the sediment transport parameter G_{gr}, the particle mobility parameter F_{gr}, and the dimensionless particle size number $D_\star$. G_{gr} is given by

$$G_{gr} = \frac{q_t}{\overline{u}D}\left(\frac{u_*}{\overline{u}}\right)^n = C\left(\frac{F_{gr}}{A_{gr}} - 1\right)^m$$

where q_t is the volumetric total transport rate per unit width (m^3/m/sec), $\overline{u}$ is the velocity of flow, D is particle size, $u_\star$ is the friction velocity, and F_{gr} is expressed as

$$F_{gr} = \frac{u_*^n}{\left[g\left(G_s - 1\right)D\right]^{1/2}}\left[\frac{\overline{u}}{\sqrt{32}\log\left(10h/D\right)}\right]^{1-n}$$

where $g \approx 9.81$ m/s^2, G_s is specific gravity of the sediment, and h is flow depth. The last parameter we need is the dimensionless particle size $D_\star$, namely

$$D_* = \left[\frac{g\left(G_s - 1\right)}{\nu^2}\right]^{1/3} D$$

where ν is the kinematic viscosity of water.

Importantly, the index n has physical significance, since its magnitude is related to $D_\star$. For fine grains, $n = 1$; for coarse grains, $n = 0$; for transitional sizes, n is a function of the base-10 logarithm of $D_\star$, that is, $n = f(\log_{10}D_\star)$. The values of n, m, A_{gr} and C are as follows:

→ For $D_\star > 60$ (coarse sediment with $D_{50} > 2$ mm):

$$n = 0 \;;\; m = 1.78 \;;\; A_{\mathrm{gr}} = 0.17 \;;\; C = 0.025$$

→ For $1 < D_\star < 60$ (transitional and fine sediment, with D_{50} in the range 0.06 – 2 mm):

$$n = 1 - 0.56\log_{10} D_*$$
$$m = 1.67 + 6.83/D_*$$
$$A_{\mathrm{gr}} = 0.14 + 0.32/D_*^{1/2}$$
$$\log_{10} C = 2.79\log D_* - 0.98\left(\log D_*\right)^2 - 3.46$$

→ *van Rijn method*

Van Rijn developed a comprehensive theory for sediment transport in rivers using fundamental physics, supplemented by empirical results. His results can be parameterized by two simple equations, one for the bed-load transport rate (q_b) and the other for suspended-load transport rate (q_s):

$$q_b = 0.005\overline{u}h\left\{\frac{\overline{u} - \overline{u}_{CR}}{\left[\left(G_s - 1\right)gD_{50}\right]^{1/2}}\right\}^{2.4}\left(\frac{D_{50}}{h}\right)^{1.2}$$

$$q_s = 0.012\overline{u}h\left\{\frac{\overline{u} - \overline{u}_{CR}}{\left[\left(G_s - 1\right)gD_{50}\right]^{1/2}}\right\}^{2.4}\left(\frac{D_{50}}{h}\right)\left(D_*\right)^{-0.6}$$

where parameter $\bar{u}_{CR}$ is determined with one of the following two equations; which one to use depends on the median diameter D_{50}:

$$\bar{u}_{CR} = 0.19\left(D_{50}\right)^{0.1} \log_{10}\left(\frac{4h}{D_{90}}\right) \quad \text{for } 0.1 \le D_{50} \le 0.5\,\text{mm}$$

$$\bar{u}_{CR} = 0.19\left(D_{50}\right)^{0.6} \log_{10}\left(\frac{4h}{D_{90}}\right) \quad \text{for } 0.5 \le D_{50} \le 2.0\,\text{mm}$$

where D_{90} is the particle size corresponding to 90% cumulative size distribution.

SOLUTIONS

P.1 ➡ *Solution*

1.False. Assuming that the wave is a deep water wave, its length is expressed as

$$L = \frac{gT^2}{2\pi} = \frac{9.81\times 8.0^2}{2\pi} = \boxed{99.92\,\text{m}}$$

Alternatively, we can appeal to the complete equation,

$$L = \frac{gT^2}{2\pi}\tanh\left(\frac{2\pi d}{L}\right)$$

$$\therefore L = \frac{9.81\times 8.0^2}{2\pi}\tanh\left(\frac{2\pi\times 120}{L}\right)$$

which can be solved with MATLAB's *fzero* function,

```
>> f = @(x) x-9.81*3^2/(2*pi)*tanh(2*pi*120/x);
>> fzero(f,100)

ans =

   99.9238
```

There is no difference between the approximate and full equations with a 2-decimal point precision.

2.True. The wave celerity is determined next,

$$C = \frac{L}{T} = \frac{99.92}{8.0} = \boxed{12.49\,\text{m/s}}$$

3.True. The wave steepness is expressed as

$$\frac{H}{L} = \frac{3.0}{99.92} = \boxed{0.0300}$$

4.False. For deep water, the particle orbits are circular, having a diameter at the surface equal to the wave height. Since a particle completes one orbit in one wave period, the particle speed at the crest would be the orbit circumference divided by the period; that is,

$$u_c = \frac{\pi H}{T} = \frac{\pi\times 3.0}{8.0} = \boxed{1.18\,\text{m/s}}$$

5.True. In order to proceed, we must first find the updated wavelength for a water depth of 12 m:

$$L = \frac{gT^2}{2\pi}\tanh\left(\frac{2\pi d}{L}\right) \rightarrow L = \frac{9.81\times 8.0^2}{2\pi}\times\tanh\left(\frac{2\pi\times 12}{L}\right)$$

Solving this transcendental equation, we have

```
>> f = @(x) x-9.81*8^2/(2*pi)*tanh(2*pi*12/x);
>> fzero(f,100)

ans =

   75.8502
```

That is, the wavelength is now updated to 75.85 m. We proceed to compute the wavenumber $k = 2\pi/L = 2\pi/75.85 = 0.0828$ m^{-1}, so that

$$n = \frac{1}{2}\left(1 + \frac{2kd}{\sinh(2kd)}\right) = 0.5 \times \left[1 + \frac{2 \times 0.0828 \times 12}{\sinh(2 \times 0.0828 \times 12)}\right] = 0.778$$

Assuming a coefficient of refraction K_r equal to 1.0, we may write

$$\frac{H}{H_0} = \sqrt{\frac{L_o}{2nL}} \underbrace{\sqrt{\frac{B_o}{B}}}_{=1} \rightarrow \frac{H}{H_0} = \sqrt{\frac{L_o}{2nL}}$$

$$\therefore H = H_0 \sqrt{\frac{L_o}{2nL}}$$

$$\therefore H = 3.0 \times \sqrt{\frac{99.92}{2 \times 0.778 \times 75.85}} = \boxed{2.76\,\text{m}}$$

6.True. The vertical velocity $w = 0$ under the wave crest. The horizontal component, in turn, is given by

$$u = \frac{\pi H}{T}\left[\frac{\cosh(k(d+z))}{\sinh(kd)}\right]\cos(kx - \sigma t)$$

But at the crest of the wave $\cos(kx - \sigma t) = 1$; also, $z = -1$, giving

$$u = \frac{\pi \times 2.76}{8.0} \times \left[\frac{\cosh(0.0828 \times (12-1))}{\sinh(0.0828 \times 12)}\right] \times 1.0 = \boxed{1.34\,\text{m/s}}$$

7.False. The wave is described by a pressure field such that

$$p = -\rho g z + \frac{\rho g H}{2}\left[\frac{\cosh(k(d+z))}{\cosh(kd)}\right]\cos(kx - \sigma t)$$

$$\therefore p = -1000 \times 9.81 \times (-1) + \frac{1000 \times 9.81 \times 2.76}{2}\left[\frac{\cosh(0.0828 \times (12-1))}{\cosh(0.0828 \times 12)}\right] \times 1.0$$

$$\therefore \boxed{p \approx 22{,}500\,\text{N/m}^2}$$

P.2 ➡ *Solution*

Part 1: Per Stokes' theory, the pertaining equation for celerity is

$$C^2 = \frac{g}{k}\tanh(kd)\left[1 + \left(\frac{\pi H}{L}\right)^2\left(\frac{9 + 8\cosh^4(kd) - 8\cosh^2(kd)}{8\sinh^4(kd)}\right)\right]$$

which, in the case of deep water, can be simplified to

$$C_0 = \sqrt{\frac{gL_0}{2\pi}\left[1 + \left(\frac{\pi H_0}{L_0}\right)^2\right]}$$

But $L_0 = C_0 T$, where T is period, so we restate the equation above as

$$C_0 = \sqrt{\frac{gC_0 T}{2\pi}\left[1 + \left(\frac{\pi H_0}{C_0 T}\right)^2\right]}$$

Substituting all available values in the right-hand side, we have

$$C_0 = \sqrt{\frac{9.81 \times C_0 \times 8.0}{2\pi} \times \left[1 + \left(\frac{\pi \times 5.0}{C_0 \times 8.0}\right)^2\right]}$$

This nonlinear equation can be easily solved with Mathematica's *FindRoot* command,

```
In[117]:= FindRoot[C0 - Sqrt[(9.81 * C0 * 8.0)/(2 * Pi) * (1 + (Pi * 5.0)/(C0 * 8.0))^2], {C0, 10}]

Out[117]= {C0 → 12.7851}
```

Thus, $C_0 \approx 12.8$ m/s. The corresponding wavelength is

$$L_0 = C_0 T = 12.8 \times 8.0 = \boxed{102\,\text{m}}$$

Note that the steepness of the wave is $H_0/L_0 = 5/102 = 0.049$, which is well below the limiting steepness of 1/7 (≈0.143). The celerity associated with small-amplitude deep water theory is given by

$$C_0 = \frac{gT}{2\pi} = \frac{9.81 \times 8.0}{2\pi} = \underline{12.5\,\text{m/s}}$$

while the wavelength is

$$L_0 = C_0 T = 12.5 \times 8.0 = \underline{100\,\text{m}}$$

Thus, Stokes' theory yields celerity and wavelength values that deviate from small-amplitude results by about 2.4 percent. It remains to compute the amplitudes of the wave crest (a_c) and trough (a_t), namely

$$a_c = \frac{H_0}{2} + \frac{\pi H_0^2}{4L_0} = \frac{5.0}{2} + \frac{\pi \times 5.0^2}{4 \times 102} = \boxed{1.44\,\text{m}}$$

$$a_t = \frac{H_0}{2} - \frac{\pi H_0^2}{4L_0} = \frac{5.0}{2} - \frac{\pi \times 5.0^2}{4 \times 102} = \boxed{1.06\,\text{m}}$$

Part 2: For the first or second order, the wavelength is expressed as

$$L_0 = \frac{gT^2}{2\pi} = \frac{9.81 \times 8.0^2}{2\pi} = 99.92\,\text{m}$$

This gives a water depth 99.92/2 = 49.96 m and a wavenumber $k = 2\pi/99.92 = 0.0629$ m^{-1}. It follows that the mass transport velocity, $\bar{u}$, becomes

$$\bar{u} = \frac{\pi^2 H^2}{2TL} \frac{\cosh\left(2k\left(d+z\right)\right)}{\sinh^2\left(kd\right)} \rightarrow \bar{u} = \frac{\pi^2 \times 5.0^2}{2 \times 8.0 \times 99.92} \times \frac{\cosh\left(2 \times 0.0629 \times \left(d+z\right)\right)}{\sinh^2\left(\pi\right)}$$

$$\therefore \bar{u} = 0.00116 \cosh\left(0.126\left(d+z\right)\right)$$

where $d + z$ is the distance up from the bottom. We can now tabulate values of $\bar{u}$ for different multiples of the wavelength L_0:

z (m)	d + z (m)	$\bar{u}$ (m/s)
0	49.96	0.314
−5.00	49.96 − 5.0 = 44.00	0.167
−9.99	39.97	0.0893
−20.0	29.96	0.0253
−30.0	19.96	0.0072
−40.0	9.96	0.0022
−50.0	≈0	0.0012

The data are plotted below. Note that mass transport velocity decays rapidly with distance below the still water level. Now, the wave celerity is given by

$$C_0 = \frac{gT}{2\pi} = \frac{9.81 \times 8.0}{2\pi} = \underline{12.5\,\text{m/s}}$$

as we have calculated in the previous problem. Using first-order crest particle velocity as sufficient for comparison purposes, we may write

$$u_c = \frac{\pi H}{T} = \frac{\pi \times 5.0}{8.0} = \underline{1.96\,\text{m/s}}$$

In summary, the wave at hand has celerity equal to 12.5 m/s, crest particle velocity equal to 1.96 m/s, and mass transport velocity at the surface equal to 0.314 m/s.

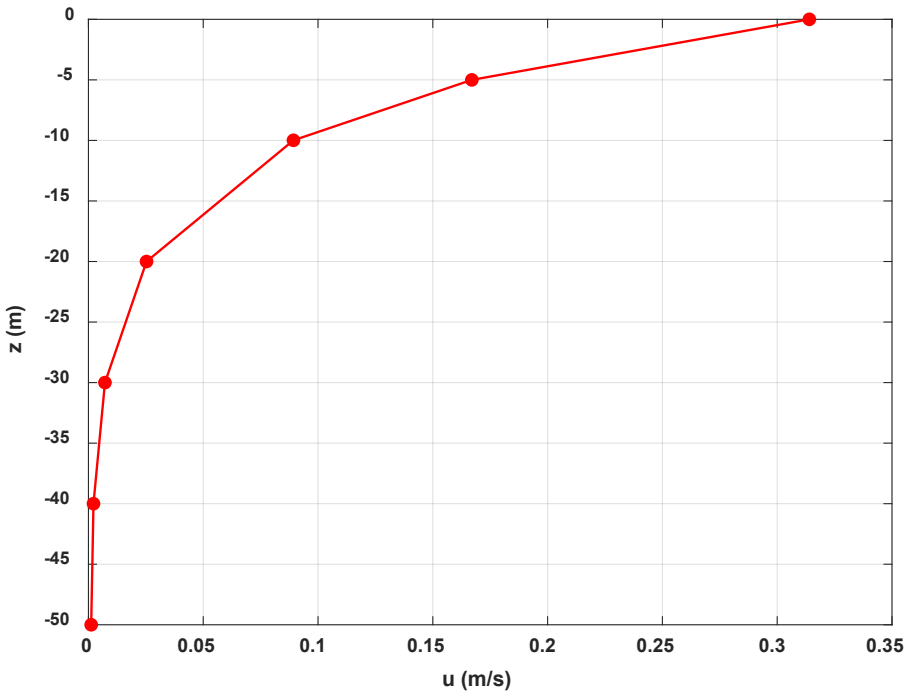

P.3 ➡ ***Solution***

Noting that the wave is a shallow water wave, its celerity is given by

$$C = \sqrt{gd} = \sqrt{9.81 \times 2} = 4.43\,\text{m/s}$$

The corresponding wavelength is

$$L = CT = 4.43 \times 12 = 53.2\,\text{m}$$

The shallow water wave approximation is reasonable if $d/L < 0.05$. In the present case, $d/L = 2/53.2 = 0.0376$, which satisfies the inequality in question. The reference celerity C_0 is, in turn,

$$C_o = \frac{gT}{2\pi} = \frac{9.81 \times 12}{2\pi} = 18.7\,\text{m/s}$$

Angle α is such that

$$\alpha = \sin^{-1}\left(\frac{C}{C_0}\sin\alpha_0\right) = \sin^{-1}\left(\frac{4.43}{18.7} \times \sin 40^\text{o}\right) = \boxed{8.76^\text{o}}$$

This is the angle between the wave crest and the shoreline at the water depth of 2 m. Next, we compute reflection coefficient K_r,

$$K_r = \sqrt{\frac{\cos\alpha_0}{\cos\alpha}} = \sqrt{\frac{\cos 40^\text{o}}{\cos 8.76^\text{o}}} = 0.880$$

This is the refraction coefficient from deepwater to the 2.0-m water depth. We proceed to compute ratio H/H_0, namely

$$\frac{H}{H_0} = \sqrt{\frac{C_o}{2nC}}\sqrt{K_r} = \sqrt{\frac{18.7}{2 \times 1.0 \times 4.43} \times 0.880} = 1.36$$

so that

$$H = 1.36H_0 = 1.36 \times 2.0 = \boxed{2.72\,\text{m}}$$

Accordingly, wave refraction decreases the wave height ($K_r < 1.0$) but the height increase caused by wave shoaling is greater, and hence there is a net increase in wave height as the wave transitions from deepwater to a point where the depth is 2.0 m.

P.4 ➡ ***Solution***

We first compute the particle size parameter $D_\star$,

$$D_* = \left[\frac{g\left(G_s - 1\right)}{\nu^2}\right]^{1/3} D \rightarrow D_* = \left[\frac{9.81\times\left(2.59-1\right)}{\left(1.4\times10^{-6}\right)^2}\right]^{\frac{1}{3}} \times\left(0.48\times10^{-3}\right)$$

$$\therefore D_* = 9.58$$

We proceed to compute coefficients n, m, A_{gr}, and C,

$$n = 1 - 0.56\log_{10}\left(D_*\right) = 1 - 0.56\times\log_{10}\left(9.58\right) = 0.450$$

$$m = 1.67 + 6.83/D_* = 1.67 + \frac{6.83}{9.58} = 2.38$$

$$A_{gr} = 0.14 + 0.23/D_*^{1/2} = 0.14 + 0.23/9.58^{1/2} = 0.214$$

$$\log_{10} C = 2.79\log_{10} D_* - 0.98\left(\log_{10} D_*\right)^2 - 3.46$$

$$\therefore \log_{10} C = 2.79\log_{10}\left(9.58\right) - 0.98\left[\log_{10}\left(9.58\right)\right]^2 - 3.46 = -1.67$$

$$\therefore C = 10^{-1.67} = 0.0214$$

and then the F_{gr} parameter,

$$F_{gr} = \frac{u_*^n}{\left[g\left(G_s - 1\right)D\right]^{1/2}}\left[\frac{\overline{u}}{\sqrt{32}\log_{10}\left(10h/D\right)}\right]^{1-n}$$

$$\therefore F_{gr} = \frac{0.2^{0.450}}{\left[9.81\times\left(2.59-1\right)\times\left(0.48\times10^{-3}\right)\right]^{1/2}}\left[\frac{2.5}{\sqrt{32}\log_{10}\left(10\times9/\left(0.48\times10^{-3}\right)\right)}\right]^{1-0.450}$$

$$\therefore F_{gr} = 1.433$$

In turn, dimensionless parameter G_{gr} is such that

$$G_{gr} = C\left|\frac{F_{gr}}{A_{gr}} - 1\right|^m = 0.0214\times\left|\frac{1.433}{0.214} - 1\right|^{2.38} = 1.345$$

Referring to the definition of G_{gr} and solving for q_t, we obtain

$$G_{gr} = \frac{q_t}{\overline{u}D}\left(\frac{u_*}{\overline{u}}\right)^n \rightarrow q_t = \frac{\overline{u}DG_{gr}}{\left(u_*/\overline{u}\right)^n}$$

$$\therefore q_t = \frac{2.5\times\left(0.48\times10^{-3}\right)\times1.345}{\left(0.2/2.5\right)^{0.450}} = 0.00503\,\mathrm{m^3/s/m}$$

$$\therefore \boxed{q_t = 5.03\times10^{-3}\,\mathrm{m^3/s/m}}$$

To use van Rijn's method, we first compute velocity $\overline{u}_{CR}$while taking $D_{90} \approx D_{50}$ = 0.48 mm in the absence of a better approximation,

$$\overline{u}_{CR} = 0.19\left(D_{50}\right)^{0.1}\log_{10}\left(\frac{4h}{D_{90}}\right) = 0.19\times\left(0.48\times10^{-3}\right)^{0.1}\times\log_{10}\left(\frac{4\times9}{0.48\times10^{-3}}\right) = 0.431\,\mathrm{m/s}$$

The bed-load contribution to sediment transport, q_b, is expressed as

$$q_b = 0.005\overline{u}h\left\{\frac{\overline{u} - \overline{u}_{CR}}{\left[\left(G_s - 1\right)gD_{50}\right]^{1/2}}\right\}^{2.4}\left(\frac{D_{50}}{h}\right)^{1.2}$$

$$\therefore q_b = 0.005\times2.5\times9\times\left\{\frac{2.5 - 0.431}{\left[\left(2.59-1\right)\times9.81\times\left(0.48\times10^{-3}\right)\right]^{1/2}}\right\}^{2.4}\times\left(\frac{0.48\times10^{-3}}{9}\right)^{1.2}$$

$$\therefore q_b = 1.71\times10^{-3}\,\mathrm{m^3/s/m}$$

The suspended-load contribution, q_s, is in turn,

$$q_s = 0.012\overline{u}h\left\{\frac{\overline{u}-\overline{u}_{CR}}{\left[\left(G_s-1\right)gD_{50}\right]^{1/2}}\right\}^{2.4}\left(\frac{D_{50}}{h}\right)\left(D_*\right)^{-0.6}$$

$$\therefore q_s = 0.012\times 2.5\times 9.0\times\left\{\frac{2.5-0.431}{\left[\left(2.59-1\right)\times 9.81\times\left(0.48\times 10^{-3}\right)\right]^{1/2}}\right\}^{2.4}\times\left(\frac{0.48\times 10^{-3}}{9.0}\right)\times 9.58^{-0.6}$$

$$\therefore q_s = 7.55\times 10^{-3}\ \mathrm{m^3/s/m}$$

Finally,

$$q_t = q_b + q_s = \left(1.71+7.55\right)\times 10^{-3} = \boxed{9.26\times 10^{-3}\ \mathrm{m^3/s/m}}$$

Van Rijn's approach leads to a total sediment load about twice as large as the load obtained through the Ackers and White approach.

P.5 ➡ *Solution*

1.False. High values of Ω (≳5 or 6) indicate much erosion of the beach by waves and hence a flat or dissipative beach. Conversely, low values (<2) indicate limited ability of waves to erode, so that the beach is more accretionary or steeper.

2.False. Christianen *et al.* (2013) actually showed that low-canopy algal cover can offer an excellent coastal-protection effect. As a result, they argue against stakeholders' lingering predilection for meadow species with high aboveground biomass.

Reference: Christianen *et al.* (2013).

3.False. Even though hard-engineering solutions have lost ground as environmental awareness grew, some Italian coastal managers and other stakeholders have advocated an increased reliance on such techniques as an alternative to beach nourishment. Indeed, it cannot be said that coastal fortification solutions and modern coastal management are irreconcilable; in a visual example, Pranzini provides a beautiful photography of Marina di Cecina, Tuscany, showing a groin that has been adapted as a walkway for beachgoers.

Reference: Pranzini (2018).

4.False. In actuality, Mull and Ruggiero (2014) concluded that the equilibrium profile model, which they denoted as KD93, most accurately reproduced the foredune retreat behavior observed in their large-scale wave tank experiment. What's more, KD93 yielded retreat distances that were bounded for low and high beach slopes. Mull and Ruggiero therefore concluded that KD93 generally performs better than either the geometric or wave impact models.

Reference: Mull and Ruggiero (2014).

5.False. Section 5 of McLachlan *et al.* (2013) provides compact case studies of their novel system as applied to 23 beaches in three continents, including each landscape's score in all six parameters that comprise the conservation value (CI) and recreation potential (RI) indices. The system offers a systematic yet simple framework for coastal stakeholders with which the choice of best management approach for a given beach can be easily drawn.

Reference: McLachlan *et al.* (2013).

6.False. Reeve's model was based on the Reynolds-averaged Navier-Stokes (RANS) framework.

Reference: Reeve *et al.* (2008).

7.False. Surprisingly, the *Rbreak* model adopted by Raubenheimer *et al.* (1995) and its associated runs led those authors to report that inclusion of sea swell could lead to greater infragravity wave energy due to a contribution of sea swell waves in the inner surf zone; on the other hand, it could also lead to *less* predicted energy in the infragravity band, consistent with increased (nonlinear) dissipation of infragravity energy owing to the sea swell energy. At any rate, in none of their model runs did the presence of sea swell cause changes in integrated infragravity energy greater than 40%, and the effect was generally lower than 20%.

Reference: Raubenheimer *et al.* (1995).

8.False. One of the reasons why Hughes actually pressed on with Wilson's (1988) approach is that it was capable of predicting the correct order of magnitude for the inferred friction factors. However, Hughes noted that Wilson's model is only valid under conditions characterized by Shields parameter θ is greater than about 0.8; in Hughes' settings at least, θ was found to be consistently above this threshold for most of the uprush motion.

Reference: Hughes (1995).

9.True. The new formula proposed by Zanuttigh and van der Meer (2008) is

$$K_r = \tanh\left(a \times \xi_0^b\right)$$

where K_r is the reflection coefficient, ξ_0 is the breaker parameter, and a and b are parameters obtained from the revetment material of the coastal structure, as listed below.

Revetment type	$\boldsymbol{a}$	$\boldsymbol{b}$
Rock permeable	0.12	0.87
Armour units	0.12	0.87
Rock impermeable	0.14	0.90
Smooth	0.16	1.43

Reference: Zanuttigh and van der Meer (2008).

10.False. Miles *et al.* (2001) acknowledge that an important limitation of their study is that data was gleaned at only one distance from the seawall. In view of the range of wave periods within the incident band of the spectrum, the instruments deployed by Miles' group were positioned within some form of moving nodal structure. For the analysis of the structure of mean flows in the nodal structure, data from one point is obviously deficient. However, for wave-driven processes such as incident wave frequency sediment suspension, one may argue that the results would hold for a large proportion of the nodal structure.

Reference: Miles *et al.* (2001) (*Modified from section 'Discussion').*

11.True. The ANN devised by Zanuttigh *et al.* (2013) consists of 13 input elements and 40 hidden neurons. This choice of hidden neuron number, Zanuttigh and her colleagues note, was warranted as a compromise between computational performance and the risk of overfitting. The ANN was found to yield reflection coefficients in excellent agreement with measured values.

Reference: Zanuttigh *et al.* (2013).

12.False. The statement errs twice, firstly by mentioning that in the Miller and Dean (2004) model the coastal environment approaches its equilibrium state linearly with time (the trend observed in most sites suggested that the process is approximately exponential), and secondly by pointing out that the model overpredicted shoreline change (it was found to be conservative in some of the sites studied).

Reference: Miller and Dean (2004).

13.True. Importantly, Yates *et al.* (2011) note that the model assumption that shoreline contour displacement depends on wave energy, rather than wave direction or alongshore gradients in waves and currents, implies that cross-shore sediment flux gradients control shoreline change.

Reference: Yates *et al.* (2011).

14.False. Aagaard and Hughes actually found that the functional relationships between bed shear stress and sediment load were reasonable, but the constants relating the two parameters were not the same for between the uprush and the backwash, and also differed with relative position in the swash zone.

Reference: Aagaard and Hughes (2006). *(Verbatim from section 6.)*

15.True. The following table lists the relative accuracy for wave-induced loads obtained with COBRAS-UC and the three semi-empirical correlations mentioned in the statement; a negative (positive) sign denotes underestimation

(overestimation). As can be seen, the code offers better accuracy and lower standard deviation than any of the correlations.

Model	Mean error	Std. Deviation
COBRAS-UC	−2.38%	±7.06%
Sainflou (1928)	−5.66%	±22.77%
Nagai (1973)	+4.25%	±22.79%
Takahashi *et al.* (1994)	+2.88%	±23.35%

Reference: Guanche *et al.* (2009).

16.True. Hubbard and Dodd (2002) used a fully adaptive mesh approach, in which high grid resolution is resorted to only where necessary, thereby reducing computational burden, and where mesh refinement is done automatically depending on the value of a user-defined parameter, thus avoiding the necessity of choosing nested grid areas beforehand for each problem.

Reference: Hubbard and Dodd (2002) (*Verbatim from p. 3).*

17.True. Indeed, in the model of Schiach *et al.* (2004) the numerical surface was consistently found to overpredict the heights of each wave. Those workers suggested that this could be attributed to the lack of dispersion within the shallow water equations when used in non-shallow water. In a similar manner, probability density functions for nonexceedance were calculated for both the physical and numerical models and compared against the expected Rayleigh distribution, and again the numerical model was found to overpredict the wave heights.

Reference: Schiach *et al.* (2004).

18.True. Part of the statement is taken verbatim from section 4.3 of Park *et al.* (2017). Park's group reported that the horizontal to vertical force ratio was low for small wave heights, indicating that for such conditions, the vertical force is larger with respect to the horizontal force and thus may be the limiting force causing structural failure. As the ratio F_H/F_V increased with respect to significant wave height, the horizontal force became larger with respect to the vertical uplift force.

Reference: Park *et al.* (2017). *(Verbatim from section 4.3).*

19.True. For those unwilling to look up the Prasad-Svendsen paper, the three problems were (1) the analytical solution of the nonlinear shallow water equations for plane-sloping beaches, which was obtained by Carrier and Greenspan in 1958; (2) the analytical solution for periodic standing waves on a plane-sloping beach, also obtained by Carrier and Greenspan in 1958; and (3) the Lagrangian finite element model for the response of harbors to long-wave excitation, as proposed by Zelt in 1986. While it is true that both the fixed grid and coordinate transformation approaches reproduced solutions to the three problems quite well, the transformation method was found to be slightly more efficient. That being said, the fixed grid method is attractive in its simplicity and probably easier to fit into large-scale simulations.

Reference: Prasad and Svendsen (2003).

20.False. The opposite is true, in that only FLOW-3D contains an AWAS. Since DualSPHysics is devoid of this feature, Altomare *et al.* (2015) advise that this code should only be used for short time series or low reflective structures.

Reference: Altomare *et al.* (2015).

21.False. Sugano *et al.* (2014) close their paper by noting that one important lesson of the 2011 Tohoku earthquake was the urgent need for coastal engineering standards and theoretical frameworks that consider the simultaneous action of earthquake motion and tsunami-wave impact. Still, it is worth noting that Japan's existing coastal infrastructure at the time of the disaster was already world-class by global standards; indeed, the country's Port and Airport Research Institute concluded that large breakwaters contributed to reduced tsunami wave heights and impeded arrival times even at locations where the waves overtopped the breakwaters.

Reference: Sugano *et al.* (2014).

22.False. Much to contrary, the strength of the Arns *et al.* (2017) study is that, through copula modelling, it correlates sea-level rise to nonlinear inputs stemming from wave heights, tides, and surges.

Reference: Arns *et al.* (2017).

23.False. Obviously, no. Cooper *et al.* (2020) actually offered a searing critique of the Vousdoukas *et al.* (2020a) paper, disapproving Vousdoukas's reliance on the Bruun rule, their omission of the nuanced nature of sea-level rise (which is such that beaches may actually prograde when the sediment budget is overwhelmingly positive), the absence of topography in the model, and the use of an arbitrary beach gradient cut-off to avoid excessive recession rates. Vousdoukas *et al.* (2020b) in turn replied to defend their methodology, arguing, for instance, that use of the Bruun rule was warranted in view of its long-established use by the coastal science community, especially in large-scale applications where data scarcity is the norm.

References: Vousdoukas *et al.* (2020a); Cooper *et al.* (2020); Vousdoukas *et al.* (2020b).

24.True. Bruun rule-based results for coastal recession, if plotted in a probability plot obtained in the PCR framework, would correspond to an exceedance probability no greater than 8%.

Reference: Ranasinghe *et al.* (2012).

REFERENCES

- Aagaard, T. and Hughes, M.G. (2006). Sediment suspension and turbulence in the swash zone of dissipative beaches. *Mar Geol*, 228(1 – 4), 117 – 135. DOI: 10.1016/j.margeo.2006.01.003
- Altomare, C., Crespo, A.J.C., Domínguez, J.M. *et al.* (2015). Applicability of Smoothed Particle Hydrodynamics for estimation of sea wave impact on coastal structures. *Coast Eng*, 96, 1 – 12. DOI: 10.1016/j.coastaleng.2014.11.001
- Arns, A., Dangendorf, S., Jensen, J. *et al.* (2017). Sea-level rise induced amplification of coastal protection design heights. *Sci Rep*, 7, 40171. DOI: 10.1038/srep40171
- Christianen, M.J.A., van Belzen, J., Herman, P.M.J. *et al.* (2013). Low-canopy seagrass beds still provide important coastal protection services. *PLoS ONE*, 8(5), e62413. DOI: 10.1371/journal.pone.0062413
- Cooper, J.A.G., Masselink, G., Coco, G. *et al.* (2020). Sandy beaches can survive sea-level rise. *Nat Clim Chang*, 10, 993 – 995. DOI: 10.1038/s41558-020-00934-2
- Guanche, R., Losada, I.J. and Lara, J.L. (2009). Numerical analysis of wave loads for coastal structure stability. *Coast Eng*, 56(5 – 6), 543 – 558. DOI: 10.1016/j.coastaleng.2008.11.003
- Hubbard, M.E. and Dodd, N. (2002). A 2D numerical model of wave run-up and overtopping. *Coast Eng*, 47(1), 1 – 26. DOI: 10.1016/S0378-3839(02)00094-7
- Hughes, M.G. (1995). Friction factors for wave uprush. *J Coast Res*, 11(4), 1089 – 98. https://www.jstor.org/stable/4298413
- MCLACHLAN, A. and DEFEO, O. (2018). *The Ecology of Sandy Shores*. 3rd edition. London: Academic Press.
- McLachlan, A., Defeo, O., Jaramillo, E. *et al.* (2013). Sandy beach conservation and recreation: Guidelines for optimising management strategies for multi-purpose use. *Ocean Coast Manag,* DOI: 10.1016/j.ocecoaman.2012.10.005
- Miles, J.R., Russell, P.E. and Huntley, D.A. (2001). Field measurements of sediment dynamics in front of a seawall. *J Coast Res*, 17(1), 195 – 206. https://www.jstor.org/stable/4300163
- Miller, J.K. and Dean, R.G. (2004). A simple new shoreline model. *Coast Eng*, 51(7), 531 – 556. DOI: 10.1016/j.coastaleng.2004.05.006
- Mull, J. and Ruggiero, P. (2014). Estimating storm-induced dune erosion and overtopping along U.S. West Coast beaches. *J Coast Res*, 30(6), 1173 – 1187. DOI: 10.2112/JCOASTRES-D-13-00178.1
- Park, H., Tomiczek, T., Cox, D.T. *et al.* (2017). Experimental modeling of horizontal and vertical wave forces on an elevated coastal structure. *Coast Eng*, 128, 58 – 74. DOI: 10.1016/j.coastaleng.2017.08.001

- Pranzini, E. (2018). Shore protection in Italy: From hard to soft engineering … and back. *Ocean Coast Manag*, 156, 43 – 57. DOI: 10.1016/j.ocecoaman.2017.04.018
- Prasad, R.S. and Svendsen, I.A. (2003). Moving shoreline boundary condition for nearshore models. *Coast Eng*, 49(4), 239 – 261. DOI: 10.1016/S0378-3839(03)00050-4
- Ranasinghe, R., Callaghan, D. and Stive, M.J.F. (2012). Estimating coastal recession due to sea level rise: beyond the Bruun rule. *Clim Change*, 110, 561 – 574. DOI: 10.1007/s10584-011-0107-8
- Raubenheimer, B., Guza, R.T., Elgar, S. *et al.* (1995). Swash on a gently sloping beach. *J Geophys Res*, 100(C5), 8751 – 8760. DOI: 10.1029/95JC00232
- REEVE, D., CHADWICK, A. and FLEMING, C. (2004). *Coastal Engineering*. London/New York: Spon Press.
- Reeve, D.E., Soliman, A. and Lin, P.Z. (2008). Numerical study of combined overflow and wave overtopping over a smooth impermeable wall. *Coast Eng*, 55(2), 155 – 166. DOI: 10.1016/j.coastaleng.2007.09.008
- Shiach, J.B., Mingham, C.G., Ingram, D.M. *et al.* (2004). The applicability of the shallow water equations for modelling violent wave overtopping. *Coast Eng*, 51(1), 1 – 15. DOI: 10.1016/j.coastaleng.2003.11.001
- SORENSEN, R.M. (2005). *Basic Coastal Engineering*. 3rd edition. Berlin/Heidelberg: Springer.
- Sugano, T., Nozu, A., Kohama, E. *et al.* (2014). Damage to coastal structures. *Soils Found*, 54(4), 883 – 901. DOI: 10.1016/j.sandf.2014.06.018
- Vousdoukas, M.I., Ranasinghe, R., Mentaschi, L. *et al.* (2020a). Sandy coastlines under threat of erosion. *Nat Clim Chang*, 10, 260 – 263. DOI: 10.1038/s41558-020-0697-0
- Vousdoukas, M.I., Ranasinghe, R., Mentaschi, L. *et al.* (2020b). Reply to: Sandy beaches can survive sea-level rise. *Nat Clim Chang*, 10, 996 – 997. DOI: 10.1038/s41558-020-00935-1
- Wilson, K.C. (1988). Frictional behaviour of sheet flow. *Progress Report 67, Institute of Hydrodynamic and Hydraulic Engineering*. Technical University of Denmark.
- Yates, M.L., Guza, R.T. and O'Reilly, W.C.O. (2009). Equilibrium shoreline response: Observations and modeling. 114(C9), C09014. DOI: 10.1029/2009JC005359
- Yates, M.L., Guza, R.T., O'Reilly, W.C.O. *et al.* (2011). Equilibrium shoreline response of a high wave energy beach. *J Geophys Res*, 116(C4), C04014. DOI: 10.1029/2010JC006681
- Zanuttigh, B. and van der Meer, J.W. (2008). Wave reflection from coastal structures in design conditions. *Coast Eng*, 55(10), 771 – 779. DOI: 10.1016/j.coastaleng.2008.02.009
- Zanuttigh, B., Formentin, S.M. and Briganti, R. (2013). A neural network for the prediction of wave reflection from coastal and harbor structures. *Coast Eng*, 80, 49 – 67. DOI: 10.1016/j.coastaleng.2013.05.004